Biosensors and Bioelectronics 24 (2009) 2643–2648

Contents lists available at ScienceDirect

Biosensors and Bioelectronics

journal homepage: www.elsevier.com/locate/bios

User-friendly, miniature biosensor flow cell for fragile high fundamental frequency quartz crystal resonators

Brigitte P. Sagmeister[a], Ingrid M. Graz[a,1], Reinhard Schwödiauer[a,*], Hermann Gruber[b], Siegfried Bauer[a]

[a] Institute of Experimental Physics, Soft Matter Physics Division, Johannes Kepler University, Altenbergerstrasse 69, 4040 Linz, Austria
[b] Institute of Biophysics, Johannes Kepler University, Linz, Austria

ARTICLE INFO

Article history:
Received 30 October 2008
Received in revised form
23 December 2008
Accepted 19 January 2009
Available online 29 January 2009

Keywords:
Quartz crystal microbalance
High frequency fundamental
Flow cell

ABSTRACT

For the application of high fundamental frequency (HFF) quartz crystal resonators as ultra sensitive acoustic biosensors, a tailor-made quartz crystal microbalance (QCM) flow cell has been fabricated and tested. The cell permits an equally fast and easy installation and replacement of small and fragile HFF sensors. Usability and simple fabrication are two central features of the HFF-QCM flow cell. Mechanical, thermal, electrical and chemical requirements are considered. The design of the cell combines these, partially contradictory, requirements within a simple device. Central design concepts are discussed and a brief description of the fabrication, with a special focus on the preparation of crucial parts, is provided. For test measurements, the cell was equipped with a standard 50 MHz HFF resonator which had been surface-functionalised with a self-assembled monolayer of 1-octadecanethiol. The reliable performance is demonstrated with two types of experiments: the real time monitoring of phospholipid monolayer formation and its removal with detergent, as well as step-wise growth of a protein multilayer system by an alternating immobilisation of streptavidin and biotinylated immunoglobulin G.

1. Introduction

During the last decade acoustic biosensors which detect mass- and viscosity-alterations of surface adsorbed biofilms via a corresponding shift in resonance frequency (Steinem and Janshoff, 2007; Bizet et al., 1999; Ballantine et al., 1997), have found widespread acceptance as versatile tools for the analysis of biomolecular interactions and related phenomena. Especially the quartz crystal microbalance (QCM) with a thickness-shear mode (TSM) resonator in combination with a flow cell is gaining increasing relevance for biological and biochemical research (Steinem and Janshoff, 2007). This trend is well reflected by the steady growth of related publications as recently reported by Cooper and Singleton (2007), who documented, for the period 2001–2005, more than 1400 articles referencing "quartz crystal microbalance" or "QCM" in the Web of Science database.

Various properties of QCM systems may account for their extensive usage. Beside the scientific merits of QCM biosensors (Marx, 2007), the principle of operation is simple and the basic elements of such a system are easily available at relatively low costs. Hence, for many research groups home made systems with a reasonable performance are easy to build and an alternative to more sophisticated, but also far more expensive commercial machines.

A crucial factor for the performance of QCM systems – home made or commercial – is the fundamental resonance frequency, f_0, of the oscillating piezoelectric sensor. A mass alteration per unit area, Δm, of a thin biofilm on the sensor surface is, to a first order approximation, the main detectable effect of biochemical binding interactions under study. It can be measured via a corresponding frequency shift, Δf, according to the Sauerbrey relation (Sauerbrey, 1959) $\Delta f = -2f_0^2/\sqrt{\rho\mu}\cdot\Delta m$, with the density $\rho = 2648\,\mathrm{g/cm^3}$, and the shear modulus $\mu = 29.47\,\mathrm{GPa}$ (AT-cut) of the quartz crystal. Since the theoretical sensitivity increases with f_0^2, the use of a sensor with a high fundamental resonance frequency is clearly desirable. Following the resonance condition $f_0 = \sqrt{\mu/\rho}/2h$, the fabrication of TSM resonators with higher values for f_0 is basically achieved by reducing the plate thickness h of the sensor.

For practical purposes however, the minimum thickness is constrained by mechanical stability issues. Most applications utilise either 5 MHz or 10 MHz resonators, with a corresponding plate thickness of 0.33 mm or 0.17 mm. Such thicknesses, in combination with a diameter of approximately 14 mm, provide a sufficient mechanical stability for an easy installation in a flow cell. Occasionally sensors with resonance frequencies between 20 MHz and 30 MHz are used (Okahata et al., 2000, 2007; Sota et al., 2002; Michalzik et al., 2005; Sota et al., 2002). These sensors are smaller in diameter (approximately 8 mm) and already rather thin and fragile. The corresponding plate thicknesses between 83 μm and 56 μm

* Corresponding author. Fax: +43 732 2468 9273.
E-mail address: reinhard.schwoediauer@jku.at (R. Schwödiauer).
[1] Present address: University of Cambridge, Nanoscience Centre, 11 JJ Thomson Ave, Cambridge, Cambridgeshire CB3 0FF, United Kingdom.

0956-5663/$ – see front matter © 2009 Elsevier B.V. All rights reserved.
doi:10.1016/j.bios.2009.01.023

require more careful handling, and also stress-free mounting to flow cells becomes increasingly difficult (Sota et al., 2002). Thus, a further improvement towards higher sensitivities may not be expected from the exploitation of even thinner standard resonators, though they are available up to about 45 MHz.

An alternate approach to higher frequencies is the utilisation of quartz resonators with an "inverted mesa" structure. These quartz disks with a diameter and thickness of about 5 mm and 0.1 mm, respectively, have a membrane of reduced thickness only in their small central circular area of about 5 mm^2. The surrounding thicker material provides a better mechanical stability and the small membrane can become as thin as 8.3 μm, resulting in a high fundamental frequency (HFF) up to $f_0 = 200$ MHz.

The first application of a 30 MHz HFF-QCM sensor in a liquid environment was demonstrated in 1993 by Lin et al. (1993) who used glucose and electrodeposited copper on the sensor surface to investigate the acoustic properties. The first application as a biosensor was presented eight years later. In a comparative study, Uttenthaler et al. (2001) investigated the detection of M13 phages in liquids and the acoustic properties of glycerol/water mixtures with four different HFF quartz crystals, operating at 39 MHz, 56 MHz, 70 MHz and 110 MHz, and with a 19 MHz standard quartz resonator. With respect to the 19 MHz standard the increase of the relative sensitivity with increasing frequency was even stronger than theoretically predicted. The 56 MHz sensor showed the best performance, with a relative improvement of the signal-to-noise ratio by a factor of 6.5 and an enhanced detection limit for phages by a factor of 200.

In spite of these encouraging results, it seems that HFF-QCM systems have still not yet appeared in research laboratories. The reason for this is rather obvious. High fundamental frequency quartz crystals are too small and, although mechanically more stable than standard resonators of equal frequency, they are still too fragile, which makes them difficult to handle and to support. Both, the small size and the fragile nature of a HFF resonator hardly allow the application of common design concepts which are frequently used for standard QCM flow cells. O-rings and electric spring contacts, as they find wide application in 5 MHz and 10 MHz systems, are not easy to down-scale. Standardised O-rings are much too hard and too bulky, electric spring contacts will find very little room to connect to the sensor and they would be tricky to fabricate. In addition, both elements will create a highly nonuniform stress distribution through the small quartz crystal and the active membrane unavoidably will be affected. It has been shown by Sota et al. (2002) that O-ring based holders for a 27 MHz quartz crystal resonator already cause less stable sensor signals. Therefore, most researchers who investigate and/or apply high frequency TSM biosensors glue the sensor irreversibly onto a larger carrier chip, e.g. see (Uttenthaler et al., 2001; Sota et al., 2002; Michalzik et al., 2005). This solution to the mounting problem actually works well, but it is very delicate, time consuming and awkward in practice. All HFF QCM sensors used in the study of Uttenthaler et al. (2001), for instance, were fabricated with bond wired crystals glued by a silicone adhesive to a carrier with open flow channels. In such a configuration the sensor crystal, once mounted, can hardly be removed from the carrier, a fact that might easily turn out to be annoying, if not problematic.

In the present work we introduce a revised version of a HFF-QCM flow cell which we have tailored to the special requirements of small and fragile HFF quartz resonators. The design allows for fast and reliable installation and replacement of a HFF sensor within a few seconds. This high user friendliness is a key feature of our system and it is accomplished without the use of complicated engineering or delicate parts. Both, the essential design guidelines and the manufacturing of crucial elements are discussed. We demonstrate the effective operation of the system with two kinds of experiments, both using a self-assembled monolayer (SAM) of 1-octadecanethiol on the gold-covered surface of a 50 MHz HFF resonator: In a first experiment we have tested the reversible functionalisation of an installed sensor by phospholipid monolayer formation from an aqueous buffer suspension of phospholipid vesicles, followed by complete lipid removal by the detergent octyl- β-D-glucopyranoside. In the second experiment, formation of an alternating protein multilayer composed of streptavidin and biotinylated immunoglobulin G was monitored.

2. Experimental

2.1. Requirements and design guidelines

The general purpose of a flow cell for QCM applications is primarily to support and connect the sensor mechanically and electrically in such a way that a flowing liquid can wet the sensitive surface in a defined region without leaking into the surrounding area. Whereas these demands are relatively easy to meet with large and stable quartz crystals, this becomes considerably more challenging for small and fragile HFF quartz resonators. For a user-friendly HFF-QCM flow cell however, there are even more requirements to specify: First, (i) the cell has to allow for fast, easy, and reliable installation and replacement of the HFF quartz sensor. Gluing or pre-wiring of the sensor shall be avoided by an effective clamping mechanism. (ii) The clamping mechanism has to act on the fragile quartz crystal with a gentle and uniform pressure; a shear-stress across the crystal must not build up. (iii) Under no circumstances, liquid must leak through the flow cell/sensor interface. Further, (iv) all materials which get in contact with the liquid have to be biologically inert. (v) All electrical lines and contacts shall be fit for high frequency signals; wires shall be short and with few discontinuities in impedance. (vi) The complete system shall be fully reusable with only little need for maintenance. Also important for a good performance are (vii) the thermal properties of the cell. A small heat capacity, in combination with a high heat conductivity, allows for fast and accurate temperature stabilisation via an external active control unit. Thermal fluctuations on the outer cell-surface shall not reach the flowing liquid, the sensor, and the probe volume. Thus, (viii) the probe volume itself shall be located in the centre, and the probe volume shall be very small, providing for fast sensor response. In addition to all these requirements, (ix) the fabrication should be inexpensive and technologically feasible even for a small workshop with conventional machine tools.

2.2. The flow cell, fabrication and assembling

All requirements mentioned above, and the related conflicting requirements of the constructions could be met and resolved with the design given in Fig. 1. For the purpose of a better illustration, the presented schematic outline is not drawn to scale and some features of small size are depicted out of proportion. A detailed exploded assembly drawing together with a complete part list and additional photographs are presented as supporting online material in Figs. S1 and S2 respectively.

The complete flow cell system measures 30 mm in diameter and 26 mm in height. The flow cell is made up of two main components: The lower flow-channel unit, which supports the HFF quartz crystal, constitutes the major part of the system. The top structure – the flow cell head – provides the high frequency signal via a planar electrode and simultaneously generates a uniform pressure upon the quartz crystal. The accurate positioning between the two parts is ensured by two precise guide bolts with threads which are tightly fixed to the lower unit and which stick through, and out of, the flow cell head, so that the two parts can be screwed together with two curled nuts on top. The quartz crystal is sandwiched in between these two parts.

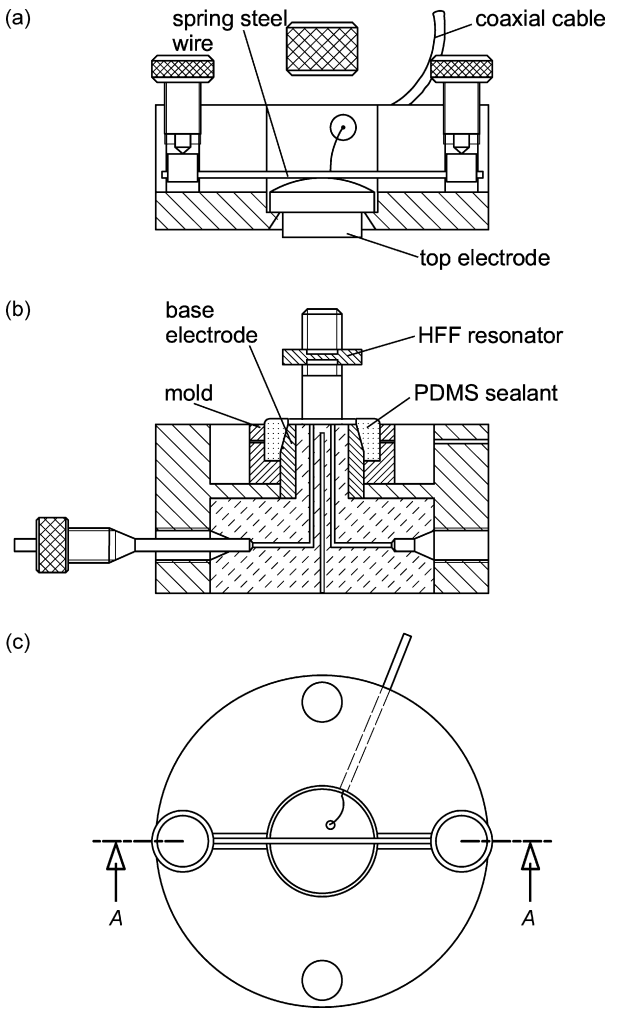

Fig. 1. Cross-sectional view from the *A–A* direction of the flow cell head (a) and the flow-channel unit with the HFF resonator above the base electrode (b) and the top view (c) of the flow cell.

The main structure of the flow cell system is made of aluminium because of its favourable thermal and electrical properties; stainless steel is used for the electrodes. The lower unit incorporates the flow cell-core, made of poly(etheretherketon) (PEEK). PEEK is chemically inert and easy to machine, it thus allowed for conventional drilling of the long and small flow channels with a diameter of 0.3 mm. The upper half of the flow cell–core, with the smaller diameter of 4 mm, is ringed by a slightly conical stainless steel tube which is also in firm contact with the main aluminium structure. This element forms the base electrode for the HFF quartz crystal. With an outer diameter of 4.5 mm, the electrode is 0.5 mm smaller than the diameter of the quartz crystal. The resulting narrow ring-area of the crystal beyond the base electrode rests on a ~50 μm elevated, soft and slightly adhesive polydimetylsiloxane (PDMS) sealant. A detailed description about the fabrication of the PDMS sealant, which is a crucial element, is given below. When the HFF quartz crystal is in full contact with the sensor platform, constituted by the PEEK surface and the coplanar base electrode, the actual flow chamber is formed by the void beneath the resonator membrane with a volume of about 0.164 μl. Only little pressure is needed to compress the PDMS; it adheres to the quartz and seals the interface effectively. The pressure on the quartz is transferred via the contact area of the upper planar electrode which exactly matches with the area of the HFF quartz crystal. A plastic insulation cap covers the planar electrode and separates it from the surrounding aluminium structure. On top, a 0.5 mm strong spring steel wire exerts a single point force on the semi-spherical insulation cap. With a space of about 0.15 mm to the surrounding aluminium, the cap is free to move and thus the ring electrode can sit on the quartz crystal with a uniform pressure. From the top electrode, the electric contact is made with a short, flexible, 50 μm thick wire to a RG 316/D coaxial cable. The outer conductor of the cable is connected to the aluminium structure. The closing of the flow cell system also closes the electric circuit.

A stable and reliable, drift-free sensor operation depends on two important criteria. The first criterion is a perfectly planar and smooth surface of the sensor platform and the top planar electrode. The second criterion is the fabrication and installation of the soft, slightly adhesive, and elevated PDMS sealant. The first step in fabrication is to cover the polished sensor platform with a thin Scotch tape. The Scotch tape must accurately match with the rim of the base electrode, the excess tape is trimmed away with the aid of a scalpel under a microscope. Afterwards the top of the flow-channel unit is covered with a thin polyimide sheet and a microscope slide which are firmly pressed against the sensor platform by two clamps. The PDMS, prepared with 2.5 vol.% of a curing agent, is injected into the mold with a syringe through the aligned filler holes. It is essential to observe the filling process under a microscope in order to see and eliminate air bubbles around the base electrode. Approximately 12 h later the microscope slide can be removed and the polyimide sheet can be stripped off carefully. The Scotch tape can then be detached with care from the sensor platform as well, and any remainders may be washed off with alcohol and a cotton bud.

At this stage, the flow cell system is ready to use. With the aid of a centreing device, e.g. a thin concentric ring, the HFF quartz crystal is exactly positioned and pressed against the adhesive PDMS. The centring device can immediately be removed and the flow cell head can be installed. Because of the weak adhesion to the PDMS, the quartz crystal can also be removed or replaced with ease at any time. A damaged or ineffective sealant can be pulled out, together with the reusable mold. After cleaning the mold and the base electrode, a new sealant can be prepared.

2.3. Flow injection analysis system

The HFF-QCM flow cell system is part of a flow injection analysis system (FIA). As schematically depicted in Fig. 2 the FIA system consists of three subunits, the active thermal control unit, the fluid transport channel unit and the measurement unit.

The active thermal control unit consists of a 70 W Peltier element which is mounted on an air-cooled radiator. The Peltier element is powered by a general purpose dual output power supply via a homemade 15 W bipolar current amplifier which is controlled by an Eurotherm 2408 PID temperature controller. The temperature of the flow cell is sensed with a type-K thermoelement which sits centrally inside the flow cell core 0.5 mm below the sensor platform. At an ambient room temperature of 21 °C a constant flow cell-temperature between 7 °C and 45 °C can be maintained with a deviation of less than ±0.05 °C.

The fluid transport channel unit comprises a Smartline 1000 HPLC pump, a Rehodyne 7725 sample injector with a sample volume of 200 μl, a 25 cm long PEEK supply capillary, and the connected flow cell. The central instrument of the measurement unit is a Hewlett Packard 4291 B impedance analyser which drives the HFF quartz crystal and measures the resonance frequency every 2.5 s. A small program on a connected computer reads, stores and displays the data in real time.

2.4. Materials

Blank HFF quartz crystals with a resonance frequency of $f_0 \approx$ 50 MHz were obtained from KVG Quartz Crystal Technology GmbH

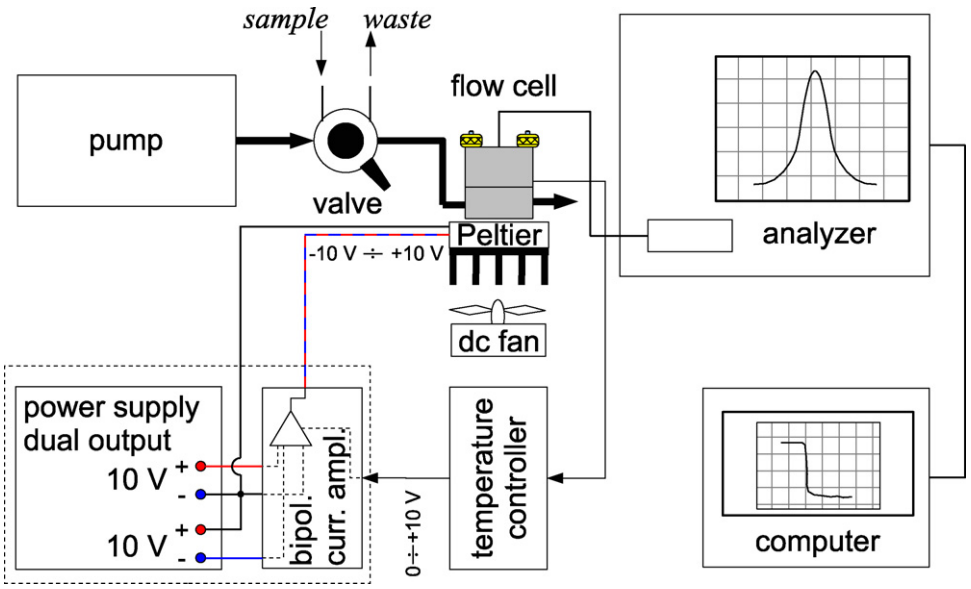

Fig. 2. Flow injection analysis system.

(http://www.kvg-gmbh.de). The measured crystal dimensions are 5 mm and 0.1 mm for the diameter and thickness of the quartz disk and 2.5 mm and 33.4 μm for the diameter and thickness of the symmetric membrane. The PDMS Silicone Elastomer, Sylgard 184, was purchased from Dow Chemical (Germany). For SAM formation on gold, 1-octadecanethiol (ODT) was obtained from Aldrich. The phospholipids 1,2-dioleoylphosphatidylcholin (DOPC), 1,2-dioloeoylphosphatidylserin (DOPS) and N-(6-biotinylamidocaproyl) 1,2-dioleoylphosphatidylethanolamin (biotin-cap-DOPE) were obtained from Avanti Polar Lipids. The detergent octyl- β-D-glucopyranoside (octylglucoside) was bought from Sigma–Aldrich. Biotinylated immunoglobolin G (IgG) antibodies with a molecular weight of 150,000 g/mol were prepared as described (Kamruzzahan et al., 2004). Streptavidin was supplied by Rockland. Phosphate-buffered saline (PBS) was prepared with water from a Milli-Q50 system (Millipore Corp., Bedford, WA) and contained 140 mM NaCl, 2.7 mM KCl, 10 mM $Na_2HPO_4$and 1.8 mM KH_2PO_4. The pH of this solution was found to be 7.3, as required and no further adjustment was necessary.

2.5. Sensor preparation

The blank HFF quartz crystal is first sonicated in ethanol. After cleaning, the crystal is put in an appropriate metal shadow mask for electrode evaporation. The shadow mask covers just the outer 0.4 mm of the quartz disk. A 70 nm Au electrode on 3 nm Cr is evaporated on both sides and all over the HFF quartz. The resulting electrode diameter of 4.2 mm will always find electrical contact to the base electrode, the remaining Au-free ring at the rim is the clean contact area for the adhesive sealant. Ideally, the metallised quartz is transferred immediately after electrode evaporation into a 1 mM ODT solution. After about twelve hours, a monolayer of ODT has self-assembled on the Au surface and the functionalised HFF sensor is removed from the ODT solution, extensively rinsed with ethanol and distilled water, dried with nitrogen gas, and installed in the flow cell, as described above.

3. Results and discussion

3.1. Performance test

The quality of the flow cell clamping mechanism is crucial for low frequency noise. It was tested by measurements of a double-sided Au-coated 50 MHz HFF resonator in the flow cell and compared with measurements of an industrially packaged 51 MHz HFF resonator in a conventional two-point mount package with removed cover. Both resonators were measured at room temperature (22 °C) under dry condition and under liquid loading with distilled, purified water. The loading of the packaged 51 MHz resonator happened with a drop of water from a syringe on its horizontal top surface. In each case the noise of the resonance frequency and the quality factor were recorded. The numerical results for the mean frequency, $\langle f_0 \rangle$, the standard deviation, σ, the maximum frequency difference, $\Delta f_{max} = f_{max} - f_{min}$, and the mean quality factor, $\langle Q \rangle$, are listed in Table 1, the corresponding figures of the frequency noise are presented in the supplementary part online with Figs. S3 and S4 (also characteristic resonance spectra are presented with Fig. S5, noise figures at different temperatures are discussed and presented with Fig. S6 and Table S2). Both resonators show very little difference in their frequency noise. The noise of the resonator in the flow cell is even a bit lower than the noise of the resonator supported by standard two-point mounting clips. This result is a good indication that the shear stress in the resonator induced by the flow cell clamping mechanism does not exceed the already low shear stress which is produced by conventional mounting clips.

It has to be mentioned, however, that the frequency noise is still considerably higher than reported by Uttenthaler et al. (2001). The reason for this notable difference may be attributed to electronic issues of our circuitry. We have used a broadband impedance analyser instead of a high quality low bandwidth oscillator circuit. Even resonators contacted stress-free with silver paste and thin gold wires did not show lower noise levels than those given in Table 1. The values mark the low resolution limit of our electronic measurement system. A specially designed oscillator circuit with

Table 1
Statistical parameters of the signal noise for a HFF resonator in the flow cell and for a HFF resonator bonded between standard two-point mounting clips in dry condition and under liquid loading (l.l.).

	$\langle f_0 \rangle$ (MHz)	σ (Hz)	Δf_{max} (Hz)	$\langle Q \rangle$
Flow cell dry	50.828	0.67	3.96	9820
Open HFF dry	51.823	0.98	6.60	28050
Flow cell l.l.	50.806	14.70	89.27	1034
Open HFF l.l.	51.795	35.25	176.00	964

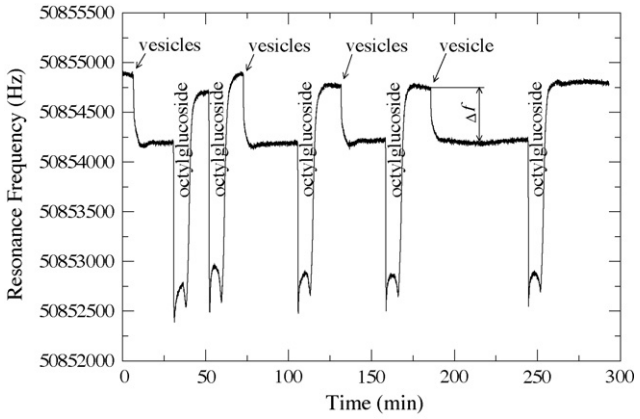

Fig. 3. Reversible functionalisation of the sensor surface with a phospholipid monolayer by alternating injection of lipid vesicles (DOPC/DOPS = 9/1, 1 mg/ml in PBS) and the detergent octylglucoside (40 mM in water).

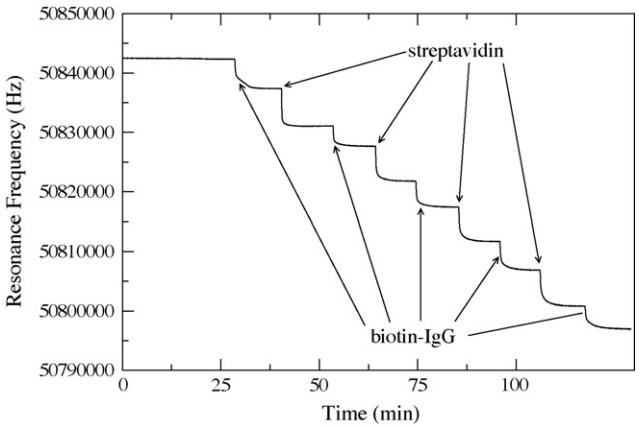

Fig. 4. Formation of protein multilayer on top of a phospholipid monolayer. Lipid vesicles (DOPC/DOPS/biotin-cap-DOPE = 70/10/20, 1 mg/ml in PBS) were injected, followed by alternating injections of streptavidin (2 μM, in PBS) and biotinylated IgG (2 μM, in PBS).

a narrow bandwidth is likely to improve the signal-to-noise ratio significantly.

3.2. Reversible functionalisation of the sensor surface with a phospholipid monolayer

The assembled HFF sensor was maintained at 22 °C and perfused with a continuous flow of PBS at a rate of 30 μl/min. In this configuration, a base line with a mean resonance frequency of about 50.8549 MHz and a standard deviation of ±10.2 Hz could be measured, the corresponding Q-factor, $Q = f_0/\Delta f_{FWHM}$, with the frequency width, Δf_{FWHM}, at the 50% value of the conductance, was about 985.

As can be seen in Fig. 3 the injection of lipid vesicles (DOPC/DOPS = 9/1, 1 mg/ml in PBS) resulted in a rapid change of the resonance frequency and after about 7 min a stable level was reached which was almost 700 Hz lower than before the injection. This process is well known to reflect the formation of a phospholipid monolayer on the hydrophobic SAM of octadecanethiol (Lingler et al., 1987). The phospholipid monolayer could perfectly be removed by injection of octylglucoside (40 mM), as regularly used to regenerate BIAcore chips with octadecanethiol SAMs (Gamsjäger et al., 2005).

The different viscosity and density of the detergent causes a strong response with a frequency shift of almost −2 kHz. After the octylglucoside injection the sensor surface is again superfused with PBS and now the resonance frequency returns to the original value from before the application of phospholipid, as previously observed for octadecanethiol-coated BIAcore chips (Gamsjäger et al., 2005). The procedure of lipid monolayer formation and its removal with detergent can be repeated many times, the sensor response is always reproducible with a frequency shift of about $\Delta f \approx -560$ Hz for the monolayer formation and ≈ −2 kHz for the response during detergent injection.

The surfactant activity of the detergent is a special challenge for the PDMS sealant. It is worth mentioning therefore, that the sealant/sensor interface was always working reliably and no leakage has been observed.

3.3. Multilayer formation

A second HFF quartz crystal was coated with 1-octadecanethiol and installed in the flow cell. The sensor was first exposed to a continuous flow of PBS at a rate of 30 μl/min for approximately 25 min and the flow cell temperature was adjusted to 23 °C. After stabilisation of the base line, a mean resonance frequency of about 50.8423 MHz and a standard deviation of ±10.2 Hz could be measured, the corresponding Q-factor was about 1007. Then a vesicle suspension with another lipid composition (DOPC/DOPS/biotin-cap-DOPE = 70/10/20, w/w/w, 1 mg/ml in PBS) was injected, resulting in monolayer formation which carried biotin residues on 20% of the phospholipid head groups. Monolayer formation was accompanied by a decrease in the resonance frequency of about −5 kHz and a stable plateau was reached within 5 min. The biotin-presenting monolayer allowed for biospecific binding of streptavidin which is a tetramer having two pairs of biotin-binding sites of which only two are used for docking to the lipid monolayer (Hahn et al., 2007). The second pair of biotin-binding sites is then available for binding of antibodies (IgG) carrying about 5–6 biotin residues per protein molecule (Kamruzzahan et al., 2004), allowing for protein multilayer formation (Hahn et al., 2007), as exemplified in Fig. 4. In consecutive steps of about 11 min a 2 μM streptavidin solution and a 2 μM biotin-IgG solution were injected. Each immobilisation caused a strong decrease in the resonance frequency. The mean frequency change is −6000 Hz for binding of a strepatavidin monolayer and −4400 Hz for each layer of biotin-IgG.

4. Conclusion

The flow cell presented in this study allows for simple and efficient use of small and fragile HFF quartz crystal resonators as high-sensitivity QCM biosensors. Any circular HFF resonator with suitable diameter can be installed and/or replaced within a few seconds. No pre-configuration like gluing, sealing or wiring is required. This high user friendliness is one of the key features of the system. It is achieved with a multifunctional clamping mechanism which proved to be robust and reliable throughout all experiments. Another advantage of the flow cell is the “low-tech” design. No sophisticated machinery or technology is necessary to fabricate all parts, including the crucial elements of the clamping mechanism.

In general, the presented flow cell demonstrates a good working concept and a first approach towards a system that makes the application of HFF quartz crystal resonators not only beneficial in terms of sensitivity but also more easily accessible, more convenient, and thus attractive for practical application.

Acknowledgments

Work supported by the Austrian Science Funds within the Translational Research Program, FFG L442-N14.

Appendix A. Supplementary Data

Supplementary data associated with this article can be found, in the online version, at doi:10.1016/j.bios.2009.01.023.

References

Ballantine, D.S., White, R.M., Martin, S.J., Ricco, A.J., Zellers, E.T., Frye, G.C., Wohltjen Jr., H., 1997. Acoustic Wave Sensors, 1st ed. Academic Press, San Diego.
Bizet, K., Gabrielli, C., Perrot, H., 1999. Analysis 7, 609–616.
Cooper, M.A., Singleton, V.T., 2007. J. Mol. Recognit. 3, 154–184.
Gamsjäger, R., Johs, A., Gries, A., Gruber, H.J., Romanin, C., Prassl, R., Hinterdorfer, P., 2005. Biochem. J. 389, 665–673.
Hahn, C.D., Leitner, C., Weinbrenner, T., Schlapak, R., Tinazli, A., Tampé, R., Lackner, B., Steindl, C., Hinterdorfer, P., Gruber, H.J., Hölzl, M., 2007. Bioconj. Chem. 18, 247–253.
Kamruzzahan, A.S.M., Kienberger, F., Stroh, C.M., Berg, J., Huss, R., Ebner, A., Zhu, R., Rankl, C., Gruber, H.J., Hinterdorfer, P., 2004. Biol. Chem. 385, 955–960.
Lingler, S., Rubinstein, I., Knoll, W., Offenhausser, A., 1987. Langmuir 26, 7085–7091.
Lin, Z., Yip, C.M., Joseph, I.S., Ward, M.D., 1993. Anal. Chem. 11, 1546–1551.
Marx, K.A., Steinem, C., Janshoff, A., 2007. Piezoelectric Sensors, 1st ed. Springer, Berlin, Heidelberg, pp. 371–424.
Michalzik, M., Wendler, J., Rabe, J., Büttgenbach, S., Bilitewski, U., 2005. Sens. Actuat. B. 105, 508–515.
Ogi, H., Motoshisa, K., Matsumoto, T.,Hatanaka, K., Hirao, M., 2006. Anal. Chem. 78, 19, 383 6903–6909.
Okahata, Y., Niikura, K., Furusawa, H., Hisao, M., 2000. Anal. Sci. 11, 1113–1119.
Okahata, Y., Mori, T., Furusawa, H., Nihira, T., 2007. In: Steinem, C., Janshoff, A. (Eds.), Piezoelectric Sensors, 1st ed. Springer, Berlin, Heidelberg, pp. 341–369.
Sauerbrey, G., 1959. Z. Phys. 155, 206–222.
Sota, H., Yoshimine, H., Whittier, R.F., Gotoh, M., Shiohara, Y., Hasegawa, Y., Okahata, Y., 2002. Anal. Chem. 74 15, 3592–3598.
Steinem, C., Janshoff, A. (Eds.), 2007. Piezoelectric Sensors, 1st ed. Springer, Berlin, Heidelberg.
Uttenthaler, E., Schräml, M., Mandel, J., Drost, S., 2001. Biosens. Bioelectron. 12, 734–735.